Bioorganic & Medicinal Chemistry Letters 23 (2013) 3325–3328

Contents lists available at SciVerse ScienceDirect

Bioorganic & Medicinal Chemistry Letters

journal homepage: www.elsevier.com/locate/bmcl

Identification of the fused bicyclic 4-amino-2-phenylpyrimidine derivatives as novel and potent PDE4 inhibitors

Taiji Goto [a,d,*], Akiko Shiina [b], Toshiharu Yoshino [a], Kiyoshi Mizukami [c], Kazuki Hirahara [a], Osamu Suzuki [a], Yoshitaka Sogawa [a], Tomoko Takahashi [a], Tsuyoshi Mikkaichi [a], Naoki Nakao [a], Mizuki Takahashi [a], Masashi Hasegawa [a], Shigeki Sasaki [d]

[a] R&D Division, Daiichi Sankyo Co., Ltd, 1-2-58 Hiromachi, Shinagawa-ku, Tokyo 140-8710, Japan
[b] Quality & Safety Management Division, Daiichi Sankyo Co., Ltd, 3-5-1 Nihonbashihoncho, Chuo-ku, Tokyo 103-8426, Japan
[c] Corporate Strategy Division, Daiichi Sankyo Co., Ltd, 3-5-1 Nihonbashihoncho, Chuo-ku, Tokyo 103-8426, Japan
[d] Graduate School of Pharmaceutical Sciences, Kyushu University, 3-1-1 Maidashi, Higashi-ku, Fukuoka 812-8582, Japan

ARTICLE INFO

Article history:
Available online 4 April 2013

Keywords:
PDE4
PDE4 inhibitor
PDE4B
cAMP
COPD
Anti-inflammatory agent
Crystallography
2-Phenylpyrimidine

ABSTRACT

2-Phenyl-4-piperidinyl-6,7-dihydrothieno[3,4-*d*]pyrimidine derivative (**2**) was found to be a new PDE4 inhibitor with moderate PDE4B activity (IC_{50} = 150 nM). A number of derivatives with a variety of 4-amino substituents and fused bicyclic pyrimidines were synthesized. Among these, 5,5-dioxo-7,8-dihydro-6H-thiopyrano[3,2-*d*]pyrimidine derivative (**18**) showed potent PDE4B inhibitory activity (IC_{50} = 25 nM). Finally, *N*-propylacetamide derivative (**31b**) was determined as a potent inhibitor for both PDE4B (IC_{50} = 7.5 nM) and TNF-α production in mouse splenocytes (IC_{50} = 9.8 nM) and showed good in vivo anti-inflammatory activity in the LPS-induced lung inflammation model in mice (ID_{50} = 18 mg/kg). The binding mode of the new inhibitor (**31e**) in the catalytic site of PDE4B is presented based on an X-ray crystal structure of the ligand–enzyme complex.

Phosphodiesterases (PDEs)[1] catalyze the hydrolysis of cyclic adenosine monophosphate (cAMP) and cyclic guanosine monophosphate (cGMP) to the corresponding nucleoside 5′-monophosphates. PDEs are responsible for the regulation of intracellular levels of cAMP and cGMP, mediating various biological responses. PDE4 specifically catalyzes the hydrolysis of cAMP and is a predominant isozyme expressed in airway smooth muscle cells as well as immune and inflammatory cells.[2] Elevation of cAMP by inhibition of PDE4 contributes to bronchodilation and suppression of inflammatory responses. Therefore PDE4 inhibitors are expected to be promising anti-inflammatory agents for the treatment of asthma, chronic obstructive pulmonary disease (COPD) and other inflammatory diseases.[3]

Roflumilast (**1**)[4] is a selective PDE4 inhibitor and the only one that has been launched as an anti-inflammatory drug for treating COPD.[5] The initial compound for our investigation is 2-phenyl-4-piperidinyl-6,7-dihydrothieno[3,4-*d*]pyrimidine derivative **2**, which moderately inhibited human PDE4B activity (IC_{50} = 150 nM)[6] and lipopolysaccharide (LPS)-induced tumor necrosis factor alpha (TNF-α) production in mouse splenocytes (IC_{50} = 620 nM).[7] As overproduction of TNF-α is associated with a number of autoimmune and inflammatory diseases, suppression of TNF-α production is thought to be a key effect of anti-inflammatory activity of PDE4 inhibitors.[8] In this Letter, we report our exploration of novel PDE4 inhibitors that have sulfur containing bicyclic structures (Fig. 1).

Initially a modification of the piperidine side chain of **2** was conducted. Preparation of derivatives is shown in Scheme 1. Starting material **3** was condensed with benzamidine **4** to give **5**. The conversion of the hydroxyl group of **5** to the chlorine substituent was performed by treatment with phosphoryl chloride to give 4-chloropyrimidine **6**. The chlorine atom of **6** was substituted with ethyl 2-(4-piperidinyl)acetate or ethyl 2-(4-aminophenyl)acetate,

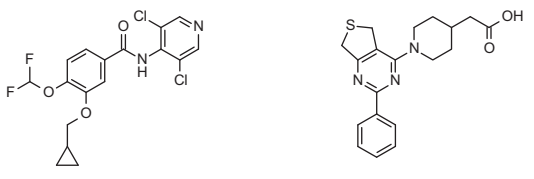

1
Roflumilast (Daxas™)
hPDE4B (IC_{50}) = 0.49 nM
mTNF-α (IC_{50}) = 1.2 nM

2
hPDE4B (IC_{50}) = 150 nM
mTNF-α (IC_{50}) = 620 nM

Figure 1. Structure of Roflumilast (**1**) and lead compound **2**.

* Corresponding author. Tel.: +81 334923131.
E-mail address: goto.taiji.kt@daiichisankyo.co.jp (T. Goto).

0960-894X/$ - see front matter © 2013 Elsevier Ltd. All rights reserved.
http://dx.doi.org/10.1016/j.bmcl.2013.03.104

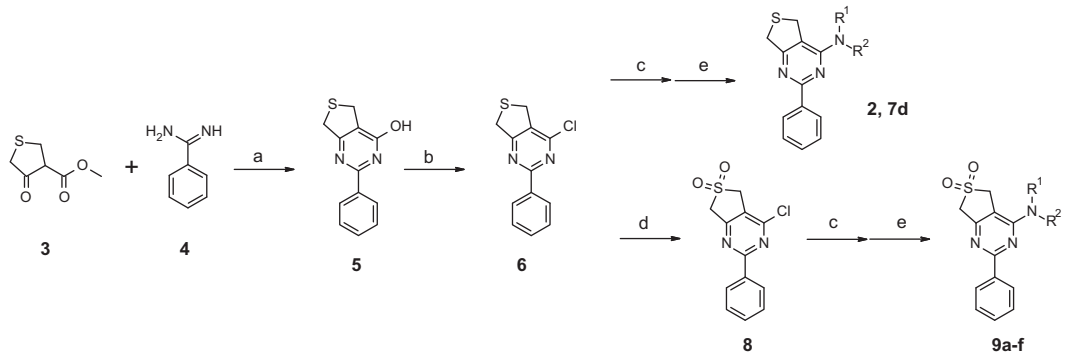

Scheme 1. Reagents and conditions: (a) NaOMe, MeOH; (b) $POCl_3$ (55% from **3**); (c) amine, DMF; (d) mCPBA, CH_2Cl_2 (53%); (e) 1 N NaOH, EtOH.

Table 1
In vitro inhibitory activity of compounds **2**, **7d**, and **9a–f**

		hPDE4B IC_{50} (nM)		hPDE4B IC_{50} (nM)
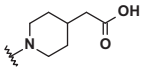	**2**	150	**9a**	190
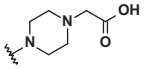	—	—	**9b**	5000
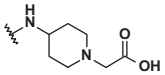	—	—	**9c**	3000
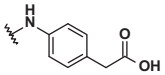	**7d**	29	**9d**	140
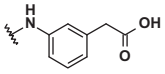	—	—	**9e**	2500
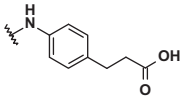	—	—	**9f**	800

and the ester group of the resulting compound was hydrolyzed to afford compounds **2** and **7d**, respectively. Intermediate **6** was oxidized to give sulfone **8**. The 4-position of pyrimidine was substituted with amines and the esters were hydrolyzed to afford compounds **9a–f**.

The results of in vitro assay are shown in Table 1. Compound **9a**, the oxidized analogue of sulfide **2**, sustained moderate PDE4B inhibitory activity, however, introduction of basic side chains was not favorable (**9b**,**c**). On the other hand, **9d** with the 2-(4-aminophenyl)acetic acid side chain showed moderate PDE4B inhibition, and sulfide **7d** exhibited good PDE4B inhibitory activity. The 2-(3-aminophenyl)acetic acid side chain and the 3-(4-aminophenyl)propanoic acid side chain decreased the potency (**9e**,**f**). These results indicated that the 2-(4-aminophenyl)acetic acid side chain is appropriate for PDE4B inhibition.

Next, we optimized the sulfide ring moiety of **7d**. The PDE4B inhibitory activities of the bicyclic derivatives are shown in Table 2. Six-membered ring compound **11** exhibited the highest PDE4B inhibitory activity in the aliphatic ring compounds (**10**–**12**). Replacement of the sulfur atom with the oxygen atom decreased the PDE4B inhibitory potency (**13**). The aromatic bicyclic derivatives, benzopyrimidine **14**, pyridopyrimidine **15** and thienopyrimidine **16**, showed lower activities than **7d**.

Further exploration of the sulfide ring moiety is shown in Table 3. Six-membered cyclic sulfide **17**, sulfone **18**, and sulfone **19** exhibited equipotent PDE4B inhibitory activity to **7d**. However, **19** did not show activity against LPS-induced TNF-α production in mouse splenocytes, probably due to its low permeability.[9] Although five-membered cyclic sulfone **20** exhibited moderate PDE4B inhibitory potency, it was inactive against the TNF-α production. Six-membered cyclic sulfone **21**, which is an isomer of **18** and **19**, showed only poor PDE4B inhibition. As a result, we could acquire the new templates, **7d**, **17**, and **18** for further investigation.

Although these new carboxylic acid compounds exhibited good PDE4B potency, their inhibitory activities against LPS-induced TNF-α production in mouse splenocytes were much weaker than that of Roflumilast (IC_{50} = 1.2 nM). While investigating more potent compounds against TNF-α production, we found that the conversion of the carboxylic acid moiety to primary amide was effective (Fig. 2). Amide **22** strongly inhibited TNF-α production with improved permeability. From this result, we conducted further exploration of amide derivatives.

Table 2
In vitro inhibitory activity of compounds **7d** and **10**–**16**

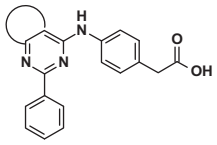

		hPDE4B IC_{50} (nM)			hPDE4B IC_{50} (nM)
7d	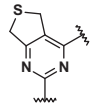	29	**13**	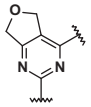	2200
10	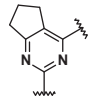	610	**14**	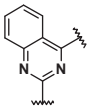	480
11	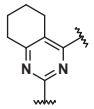	430	**15**	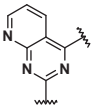	14%[a]
12	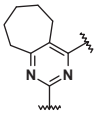	35%[a]	**16**	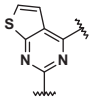	230

[a] inhibition % at 10 μM.

Table 3
In vitro profile of compounds **7d**, **9d**, and **17**–**21**

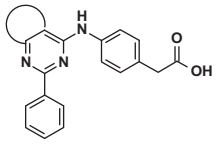

		hPDE4B IC_{50} (nM)	mTNF-α IC_{50} (nM)	Log *D*[a] (pH 7.4)	PAMPA Pe[b] (10^{-6} cm/sec) (pH 7.4)
7d	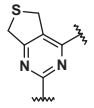	29	220	1.3	13.3
9d	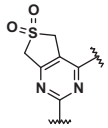	140	970	0.016	<2.0
17	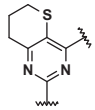	29	90	1.4	15.5
18	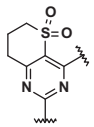	25	390	0.43	5.8
19	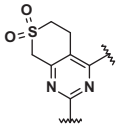	28	>10 μM	−0.45	<2.0

Table 3 (*continued*)

		hPDE4B IC_{50} (nM)	mTNF-α IC_{50} (nM)	Log *D*[a] (pH 7.4)	PAMPA Pe[b] (10^{-6} cm/sec) (pH 7.4)
20	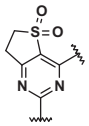	280	>10 μM	NT	NT
21	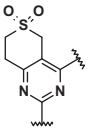	7900	NT	NT	NT

[a] Distribution coefficient.[6]
[b] Permeability coefficient in parallel artificial membrane permeability assay.[9]

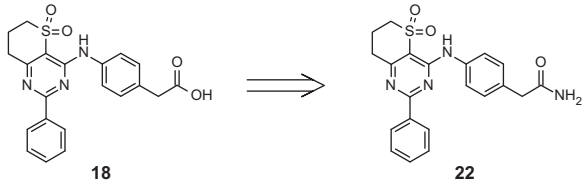

18
hPDE4B (IC_{50}) = 25 nM
mTNF-α (IC_{50}) = 390 nM
Log D (pH 7.4) = 0.43
PAMPA (pH 7.4)
Pe (10^{-6} cm/sec) = 5.8

22
hPDE4B (IC_{50}) = 16 nM
mTNF-α (IC_{50}) = 8.5 nM
Log D (pH 7.4) = 2.9
PAMPA (pH 7.4)
Pe (10^{-6} cm/sec) > 50

Figure 2. Comparison of **18** and **22**.

The amide derivatives (**22**, **31a**–**h**) were prepared as shown in Scheme 2. Starting material **23** was reacted with methyl thioglycolate **24** to give **25**. Dieckmann condensation of **25** afforded a mixture of desired **26a** and its isomer **26b**. The mixture of **26a** and **26b** was condensed with benzamidine to give the pyrimidine intermediate **27a** and **27b** (**27a**:**27b** = 8:1). After conversion to the triflate **28a** and **28b**, these two isomers were separated. Oxidation of **28a** afforded the sulfone **29**, which reacted with ethyl 2-(4-aminophenyl)acetate to give **30**. Hydrolysis of **30**, followed by condensation with various amines provided the amide derivatives (**22**, **31a**–**h**).

As shown in Table 4, Linear alkyl, branched alkyl and aryl substituted compounds were synthesized (**31a**–**h**). These amide derivatives achieved significant enhancement of activities against LPS-induced TNF-α production in mouse splenocytes. Particularly, **31f** showed higher potency than Roflumilast.

Some of these amide derivatives were evaluated in in vivo inhibitory activity against LPS-induced pulmonary neutrophilia in mice.[10] In this model, **31b** exhibited high efficacy with an ID_{50} = 18 mg/kg (ip), and **31c** was also effective with an ID_{50} = 23 mg/kg (ip). On the other hand, **31f** was not efficacious, although the reason is unclear.

For further consideration of SAR, an X-ray crystal structure of **31e** in PDE4B was obtained (Fig. 3).[11] The nitrogen atom of pyrimidine interacts with Glu443 and the oxygen atoms of the sulfone form the hydrogen bonding network to Tyr233 and Asn395 via water molecules. The aliphatic moiety of the sulfone ring occupies a lipophilic pocket similar to the difluoromethoxy moiety of Roflumilast.[12] The side chain of **31e** forms a bending conformation and the tertiary butyl group occupies a lipophilic pocket composed of Phe414, Met431 and Phe506. These interactions presumably contribute to high PDE4B inhibitory activity of **31e**.

In summary, we identified a series of novel PDE4 inhibitors that have a 4-amino-2-phenylpyrimidine core fused with sulfur contained rings. These compounds showed high in vitro PDE4B

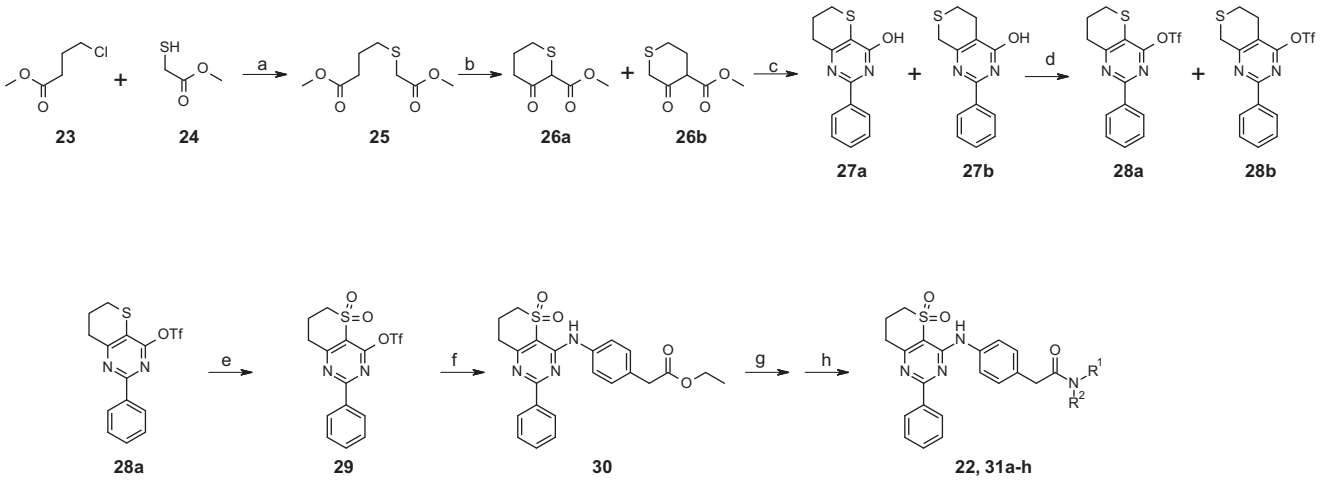

Scheme 2. Reagents and conditions: (a) NaOMe, NaI, MeOH; (b) NaOMe, toluene; (c) benzamidine, NaOMe, MeOH; (d) Tf_2O, NEt_3, DMAP, CH_2Cl_2 (43% for **28a**, 5% for **28b**, 4 steps); (e) mCPBA, CH_2Cl_2 (98%); (f) ethyl 2-(4-aminophenyl)acetate, DMF; (g) 1 N NaOH, EtOH; (h) amine, WSC, HOBt, DIPEA, DMF.

Table 4
In vitro inhibitory activity of **22** and **31a–h**

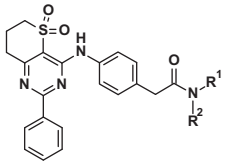

	R^1	R^2	hPDE4B IC_{50} (nM)	mTNF-α IC_{50} (nM)
22	H	H	16	8.5
31a	Methyl	H	27	35
31b	*n*-Propyl	H	7.5	9.8
31c	*n*-Butyl	H	22	13
31d	*i*-Butyl	H	6.6	4.7
31e	*t*-Butyl	H	11	8.5
31f	Neopentyl	H	4.7	0.80
31g	Phenyl	H	43	18
31h	Methyl	Methyl	33	17
Roflumilast			0.49	1.2

inhibitory activity. Furthermore, we found that the amidation of the 2-(4-aminophenyl)acetic acid moiety strongly enhanced inhibitory activity against LPS-induced TNF-α production in isolated mouse splenocytes. Among these compounds, **31b** and **31c** exhibited high in vivo efficacy in the lung inflammation model in mice. Further investigation of this series of potent PDE4 inhibitors is now underway.

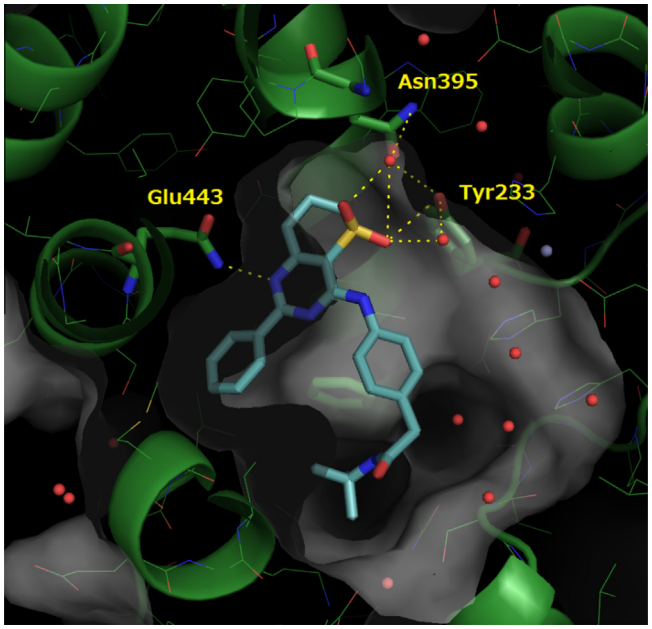

Figure 3. X-ray crystal structure of **31e** with human PDE4B catalytic binding site.[11]

Acknowledgement

We thank Professor Soichi Wakatsuki of the Institute of Materials Structure Science for the use of the facilities at the Photon Factory and technical staff for their excellent support in the use of the beamlines.

Supplementary data

Supplementary data associated with this article can be found, in the online version, at http://dx.doi.org/10.1016/j.bmcl.2013.03. 104.

References and notes

1. (a) Bender, A. T.; Beavo, J. A. *Pharmacol. Rev.* **2006**, *58*, 488; (b) Torphy, T. J. *Am. J. Respir. Crit. Care Med.* **1998**, *157*, 351.
2. Kodimuthali, A.; Jabaris, S. L.; Pal, M. *J. Med. Chem.* **2008**, *51*, 5471.
3. (a) Huang, Z.; Mancici, J. A. *Curr. Med. Chem.* **2006**, *13*, 3253; (b) Houslay, M.; Schafer, P.; Zhang, K. Y. J. *Drug Discovery Today* **2005**, *10*, 1503.
4. (a) Rabe, K. F. *Br. J. Pharmacol.* **2011**, *163*, 53; (b) Cazzola, M.; Picciolo, S.; Matera, M. G. *Expert Opin. Pharm.* **2010**, *11*, 441; (c) Giembycz, M. A.; Field, S. K. *Drug Des. Dev. Ther.* **2010**, *4*, 147.
5. (a) Pages, L.; Gavalda, A.; Lehner, M. D. *Expert Opin. Ther. Pat.* **2009**, *19*, 1501; (b) Spina, D. *Br. J. Pharmacol.* **2008**, *155*, 308.
6. hPDE4B(152–564) was cloned, expressed and purified according to the reported protocols: (a) Zhang, K. Y. J.; Card, G. L.; Suzuki, Y.; Artis, D. R.; Fong, D.; Gillette, S.; Hsieh, D.; Neiman, J.; West, B. L.; Zhang, C.; Milburn, M. V.; Kim, S. H.; Schlessinger, J.; Bollag, G. *Mol. Cell* **2004**, *15*, 279; (b) hPDE4B assay: See the Supplementary data.
7. Mouse TNF-α production assay: See the Supplementary data.
8. Castro, A.; Jerez, M. J.; Gil, C.; Martinez, A. *Med. Res. Rev.* **2005**, *25*, 229.
9. The membrane permeability coefficients were assayed using PAMPA Evolution™ (pION Inc., MA, USA). See the Supplementary data.
10. In vivo assay: See the Supplementary data.
11. The X-ray crystallographic studies were accomplished based on the procedure described in Ref. 6a The coordinate and statistics are available from the protein data bank using accession code 3W5E (complex with compound **31e**).
12. Card, G. L.; England, B. P.; Suzuki, Y.; Fong, D.; Powell, B.; Lee, B.; Luu, C.; Tabrizuzad, M.; Gillette, S.; Ibrahim, P. N.; Artis, D. R.; Bollag, G.; Milburm, M. V.; Kim, S. H.; Schlessinger, J.; Zhang, K. Y. J. *Structure* **2004**, *12*, 2223.